Int. J. Electrochem. Sci., 13 **(2018)** 11986 – 11999, doi: 10.20964/2018.12.81

International Journal of
ELECTROCHEMICAL
SCIENCE
www.electrochemsci.org

Influence of Cutting Fluids on the Corrosion Resistance of X20Cr13 Martensitic Stainless Steel

Tihana Kostadin[1,*], *Goran Cukor*[2], *Zoran Jurković*[2]

[1] Karlovac University of Applied Sciences, Ivana Meštrovića 10, 47000 Karlovac, Croatia
[2] University of Rijeka, Faculty of Engineering, Vukovarska 58, 51000 Rijeka, Croatia
[*]E-mail: tihana.kostadin@vuka.hr

Received: 9 September 2018 / *Accepted:* 11 October 2018 / *Published:* 5 November 2018

Martensitic stainless steels are difficult-to-cut materials, so the utilization of the cutting fluids with high flow rates is considered necessary in their machining. However, flood cooling method represents a high risk to human health and environment and is also a great economic burden. A chilled jet of compressed air is one of the possible alternatives to conventional liquid coolants. As corrosion can occur even in dry machining, the aim of this paper was to investigate the feasibility of replacing conventional emulsion coolant with the chilled air out of Ranque-Hilsch counter-flow vortex tube. An important outcome of corrosion testing showed a beneficial effect of the chilled air-cooling method on the corrosion resistance since it is on increase over a prolonged time. As expected, the feed rate *f* was confirmed to be the most important factor affecting the *Ra*, but the most interesting finding was that about non-significant influence of the cooling method on reducing the *Ra* and consequently on increasing the corrosion resistance of machined surface. Therefore, the chilled air-cooling by a vortex tube can be successfully applied to turning of steel X20Cr13, thereby eliminating the ecological load caused by the application of conventional liquid coolant.

Keywords: martensitic stainless steel; corrosion resistance; cooling; electrochemical and gravimetric measurements.

1. INTRODUCTION

High degree of work hardening rate, low thermal conductivity and tendency to form long chips and built up edge, which lead to bad surface finish designate stainless steels as difficult-to-cut materials. Accordingly, it is considered necessary to use the cutting fluid with high flow rate in machining of stainless steels [1]. However, after machining it is compulsory to remove all cutting fluid traces to allow the self-passivation of surface. Besides, the cutting fluids have a limited life span and upon completion of use, they should be disposed of properly.

Disposal of used cutting fluid quantities opens up numerous ecological issues, especially when taken into account that it is one of the most complex types of waste with a high organic charge [2]. It is worrying that almost 30% of the annual consumption of cutting fluids is removed from the machining system observing losses such as evaporation, uncontrolled leakage and residual quantities at the workpiece, tool or chip [3]. Handling of cutting fluid poses a risk to human health and the possibility of illness from various diseases, most commonly skin diseases [4] and malignant and non-malignant respiratory diseases [5]. Other hazardous effects are oil vapour effect, bactericidal effect, genotoxic effect, generation of carcinogenic substances [6], presence of heavy metal particles in additives, etc. The risks of using cutting fluids for the environment and human health stress the necessity for exploring the new possibilities of replacing the conventional emulsion cooling with alternative one.

The ratio of the purchasing cost and the hidden cost, which includes the individual costs of all phases of the cutting fluid life cycle, varies from 1.0 : 1.5 up to 1.0 : 5.5 [7]. Consumption in thousands of tons and allocations in billions of dollars reflect the scope and costs of using cutting fluids [8]. For difficult-to-cut materials, the cost of using cutting fluid ranges from 20% to 30% of total machining cost [9]. Hence, the high cost burden that is generated by the application of cutting fluids is another aspect that has to be taken into account.

The need to observe the application of cutting fluid from three aspects, ecological, sociological and economic, is a major challenge for researchers in seeking for better cooling and lubrication solutions in machining. At the same time, these solutions should be technically and economically competitive and should not be a threat to the future or sustainability of machining.

By using a chilled jet of compressed air, some functions of conventional cutting fluid can be replaced, from which the basic ones are cooling of the tool and workpiece as well as removal of the chips from the cutting zone. Chilled air is considered efficient in heat dissipation i.e. in lowering temperature in the cutting zone during machining. As a disadvantage, the absence of lubrication function should be mentioned. It is possible to compensate this function with the selection of special tools coated with self-lubricating coatings, which allow unobstructed cutting under such machining conditions [10].

Chilled air-cooling is most often carried out using a vortex tube, which splits a compressed air in two streams: hot (up to 100°C) and cold (down to -50°C). The latter is jetted directly to the cutting zone. Using the air as cooling medium in machining represents the cleanest and most favourable cooling method for the environment and humans [11]. Besides, the reduction in variable costs of machining due to non-use of conventional liquid coolants, easier recycling of uncontaminated chip and avoiding degreasing of workpiece after completion of machining meets today's economic demands placed in front of the machining industry.

A limited number of publications can be found on the application of chilled air-cooling in turning operations. Liu and Chou [12] revealed the benefits of chilled air-cooling at turning of hypereutectic Al-Si alloys in competition with dry machining, especially due to the reduction of tool wear and cutting force. Su et al. [13] came up with data on drastic reduction in tool wear and surface roughness, and significant improvement in chip shape in comparison to dry machining after testing the chilled air-cooling at finish turning of Inconel 718. Boswell [14] found that the effect of cooling very similar to conventional liquid coolants as well as better machining result regarding the surface

roughness and tool life relative to dry machining can be achieved by employing a vortex tube cooling system at turning of AISI 1040 carbon steel. Sharma et al. [15] provided an overview of various air-cooling techniques, which contribute to a significant improvement of productivity at turning of difficult-to-cut materials such as nickel alloys or titanium. Liu et al. [16] made a comparison of dry machining and chilled air-cooling at the hard turning of Ti6Al4V alloy, and recorded a considerably lower cutting temperature and a lower tool wear and surface roughness for the latter.

Foltz [17] stated that corrosion could occur even in dry machining and not only owing to utilization of water miscible cutting fluids. Also, in the stainless steels family, martensitic ones are the most sensitive to the appearance of corrosion. As can be seen from the above literature survey, the use of chilled air-cooling when turning martensitic stainless steels was not explored before this paper. The goal set herein was to investigate the feasibility of replacing conventional emulsion coolant with chilled air, also considering the corrosion resistance property of the selected martensitic stainless steel after the turning operation. The findings encourage such replacement so that the ecological and economical loads caused by the common application of liquid cutting fluids can be successfully eliminated. This is an important contribution on the road to "green production".

2. EXPERIMENTAL

2.1. Test Material and Machining System Setting

Material selected for testing was martensitic stainless steel X20Cr13 (EN-Nr 1.4021). Chemical composition and mechanical properties are presented in Table 1 and Table 2 respectively.

Table 1. Determined chemical composition (wt%) of X20Cr13.

Fe%	C%	Si%	Mn%	P%	S%	Cr%	Mo%	Ni%	V%	Nb%	Cu%
85.85	0.236	0.352	0.683	0.044	0.023	11.97	0.125	0.299	0.053	0.07	0.195

Table 2. Determined mechanical properties of X20Cr13 at room temperature.

Yield strength $R_{p(0.2)}$ [MPa]	Tensile strength R_m [MPa]	Elongation A [%]	Impact energy KCU [J]	Hardness [HB]
750	881	16.36	15	272

The external turning experiments on the round bars of dimensions Ø80 mm × 463 mm were carried on CNC research lathe TU 360 Prvomajska. A tool arrangement comprising a SECO cutting insert DNMG 150608-MF-4 TP 2501 and a tool holder PDJNL 2525M15 was employed. A new cutting edge was utilised for each experiment.

In the flood cooling method, INA BU 7 emulsion concentrate was used as the cutting fluid. The

concentrate content in water was 5%. In the chilled air-cooling method, a Ranque-Hilsch vortex tube with counter-flow (Nex Flow^{TM} Frigid-X Cooler System c/w 57025AD) was applied to cool and jet the compressed air into the cutting zone. The inlet air pressure of 0.69 MPa and outlet air temperature of -10°C were set as operating parameters.

2.2. Electrochemical Measurements

For electrochemical testing two specimens were machined from the test material: one applying the flood cooling method and the other applying the chilled air-cooling method. For both, CNC turning was executed with the cutting speed v_c = 220 m/min, feed rate f = 0.3 mm/rev and depth of cut a_p = 0.4 mm.

Electrochemical measurements were performed with PARSTAT 2263 potentiostat equipped with Electrochemistry PowerSuite software. A basic polarization cell was used consisting of 3.5% NaCl aqueous solution as electrolyte, a X20Cr13 working electrode (one for each specimen) with an immersed area of 1 cm^2, a saturated calomel electrode as reference electrode and a counter electrode made of graphite. Two studies were conducted: open circuit potential measurements to investigate the corrosion tendencies and potentiodynamic polarization measurements to determine the instantaneous corrosion rates of the specimens in the given medium [18].

The corrosion potential E_{corr} and the corrosion current density j_{corr} can be found from the potentiodynamic polarization measurements using the Tafel extrapolation method [19]. When determined properly, j_{corr} reflects an instantaneous corrosion rate CR_E in mm/year at the time of measurement according to equation given in ASTM Standard G102-89 [20]:

$$CR_E = 3.27\times10^{-3} EW j_{corr} / \rho \qquad (1)$$

where EW is the equivalent weight in g (here EW = 26.65 g) and ρ is the density in g/cm^3 (here ρ = 7.74 g/cm^3) of tested material X20Cr13. Described procedure is performed for both specimens.

2.3. Gravimetric Measurements

Two specimens were prepared as for electrochemical measurements and immersed in the electrolyte of the same composition. The specimens were weighed prior to the tests and after 14 days of immersion. Assuming uniform (general) corrosion, the time-averaged corrosion rate CR_G in mm/year was calculated using the equation given in ASTM Standard G1-03 [21]:

$$CR_G = 3.65\times10^{3} \Delta m / (A_s t \rho) \qquad (2)$$

where Δm is the mass loss in g, t is the immersion time in days and ρ is the density in g/cm^3.

2.4. SEM/EDS Testing

Scanning Electron Microscopy coupled with Energy Dispersive X-ray Spectroscopy (SEM/EDS) was applied to determine the surface elemental composition of the specimens after corrosion testing. Specimens were analysed by VEGA TS 5136 MM microscope and Oxford Instruments Si(Li) INCA X-sight device.

2.5. Machinability Testing

The lesser the surface roughness value, the better is the corrosion resistance. This fact is relevant when comparing different cooling methods in martensitic stainless steel turning due to the resistance of the machined surface to corrosion.

In this study, the cooling method, cutting speed v_c, feed rate f and depth of cut a_p were selected as the control factors. The cooling method was designated on two levels (flood cooling with emulsion and chilled air-cooling), whereas the other control factors were on three levels as shown in Table 3.

Table 3. Control factors in turning of X20Cr13 and their levels.

Symbol	Control factors	Level 1	Level 2	Level 3
A	Cooling method	Emulsion	Chilled air	-
B	Cutting speed v_c [m/min]	170	220	270
C	Feed rate f [mm/rev]	0.2	0.3	0.4
D	Depth of cut a_p [mm]	0.3	0.4	0.5

For the specified control factors and their levels, standard L_{18} Taguchi orthogonal array was selected as the most appropriate. Hence, 18 experiments were made. The surface roughness parameter *Ra* (mean roughness) was measured using the Hommel Tester T1000 profilometer. The *Ra* values were directly measured on the workpiece held between the chuck and tailstock, without removing it from the lathe, to avoid possible mistakes due to re-clamping operation. Also, to reduce the deviation, the average value of three measurements was taken as a result.

The obtained *Ra* data were converted to the signal-to-noise (S/N) ratios in dB to measure the performance characteristics of the levels of control factors against the desired low *Ra*. The smaller-the-better criterion was expressed as follows [22]:

$$S/N = -10 \log_{10}\left(n^{-1} \sum_{i=1}^{n} y_i^2\right) \quad (3)$$

where n is the number of replicated measurements in an experiment (here n = 1) and y_i is the measured value. Taguchi method was followed by the analysis of variance (ANOVA) to determine the statistical significance and percentage contribution of each control factor to the *Ra* change. ANOVA was performed at confidence level of 99%.

3. RESULTS AND DISCUSSION

3.1. Electrochemical Results

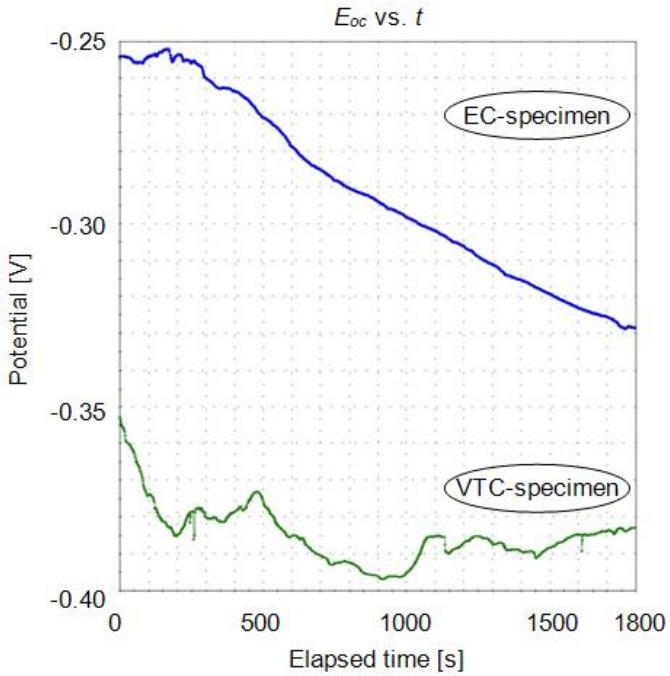

Figure 1. Open circuit potential curves of the emulsion cooled (EC) and the vortex tube cooled (VTC) X20Cr13 specimens in 3.5% NaCl aqueous solution at 25°C.

For the emulsion cooled or EC-specimen and the vortex tube cooled or VTC-specimen immersed in 3.5% NaCl aqueous solution at 25°C, the quasi-stationary E_{oc} values have been reached after 1800 s. The summary E_{oc}-t plot and recorded E_{oc} values are presented in Figure 1 and Table 4 respectively.

Table 4. Open circuit potential values obtained from open circuit potential curves.

Specimen	Initial E_{oc}	E_{oc} after 900 s	E_{oc} after 1800 s
EC	-254.3 mV	-294.0 mV	-328.6 mV
VTC	-352.8 mV	-396.2 mV	-383.0 mV

From the E_{oc} curves a comparison between the two specimens during an external longitudinal turning operation can be carried out. There is a clear evidence of the effect of the cooling method through the variation of E_{oc}. The EC-specimen shows the quasi-stationary E_{oc} value closer to zero, and thus the better corrosion properties compared to the VTC-specimen. However, the E_{oc} curve of EC-specimen tends to fall. The cause of this occurrence is the presence of an oil film, which after some time is decayed and after that the corrosion resistance of the EC-specimen decreases. The VTC-specimen shows a slight decrease in the E_{oc} curve at the beginning and then, after some time, it tends to increase towards the noble direction.

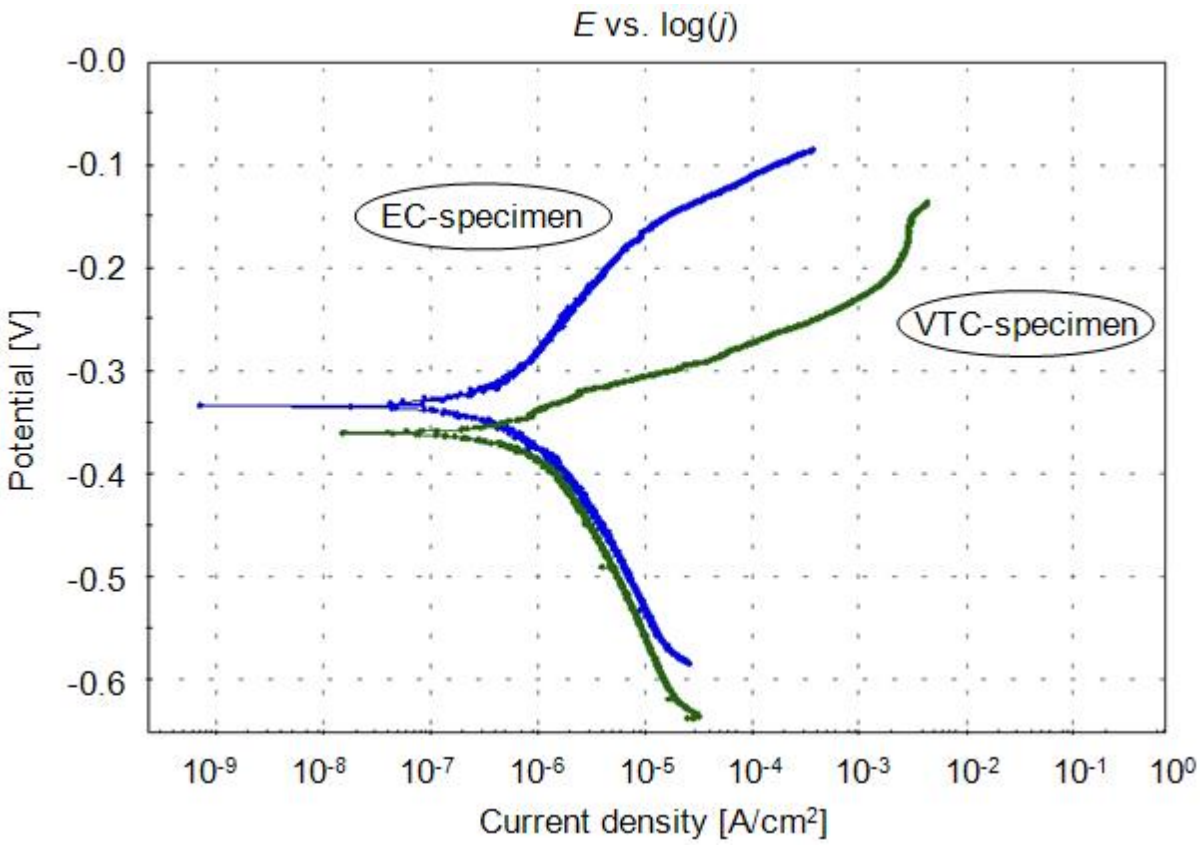

Figure 2. Potentiodynamic polarization curves of the emulsion cooled (EC) and the vortex tube cooled (VTC) X20Cr13 specimens in 3.5% NaCl aqueous solution at 25°C (scan rate 0.166 mV/s).

This result indicates a phenomenon of depassivation-passivation. There appears to be delayed spontaneous creation and gradual thickening of the passive oxide film (i.e. protective layer) on the VTC-specimen surface and the corrosion resistance is on increase over a longer time period.

Potentiodynamic polarization curves obtained at a scan rate of 0.166 mV/s are presented in the semi-logarithmic plot in Figure 2. For each specimen, the main parameters of the corrosion process i.e. the slopes b_a and b_c of anodic and cathodic Tafel lines, corrosion potential E_{corr} and corrosion current density j_{corr} were extracted from the belonging curve by Electrochemistry PowerSuite software.

The obtained data and calculated corrosion rates CR_E from Equation (1) are given in Table 5.

Table 5. Tafel data and calculated corrosion rates.

Specimen	b_a [mV/decade]	b_c [mV/decade]	E_{corr} [mV]	j_{corr} [μA/cm^2]	CR_E [mm/year]
EC	131.6	153.7	-332.7	0.555	0.00625
VTC	116.9	238.2	-359.7	1.533	0.01726

Regarding the Tafel slopes b_a and b_c it should be pointed out that an alloy with a tendency towards passivation will have $b_a > b_c$ while an alloy that corrodes will have $b_a < b_c$ [23]. The values of b_a and b_c in Table 5 indicate that both specimens reveal a tendency towards depassivation. Also, the

determined values of E_{corr} are smaller than those corresponding to E_{oc} in Table 4. This is expected with the occurrence of a depassivation phenomenon on the surface during cathodic scanning [24]. The EC-specimen exhibits greater value of E_{corr} than the VTC-specimen, thus demonstrating a lower predisposition to undergo corrosion. The value of j_{corr} is considerably lower for the EC-specimen. Since the values of CR_E are directly proportional to the values of j_{corr}, the VTC-specimen displays higher corrosion rate.

3.2. Comparison of Gravimetric and Electrochemical Corrosion Rates

Mass loss measurement generally gives a true corrosion rate occurring during specimen exposure to electrolyte. For the tested specimens, the mass losses after 14 days of immersion as well as calculated corrosion rates CR_G from Equation (2) can be found in Table 6. It can be seen that EC-specimen is more corrosion resistant in 3.5% NaCl aqueous solution at 25°C than VTC-specimen.

Table 6. Gravimetric corrosion rates after 14 days in 3.5% NaCl aqueous solution at 25°C.

Specimen	Initial mass [g]	Δm [g]	CR_G [mm/year]
EC	4.5307	0.0059	0.036
VTC	4.4051	0.0078	0.048

Corrosion rate obtained by mass loss measurement is total corrosion rate and obtained by Tafel method is momentary corrosion rate. Hence, the gravimetric corrosion rate can be substantially different from the electrochemical corrosion rate. The difference may arise ordinarily due to time effects and unusually due to errors made in determining the corrosion current density [25].

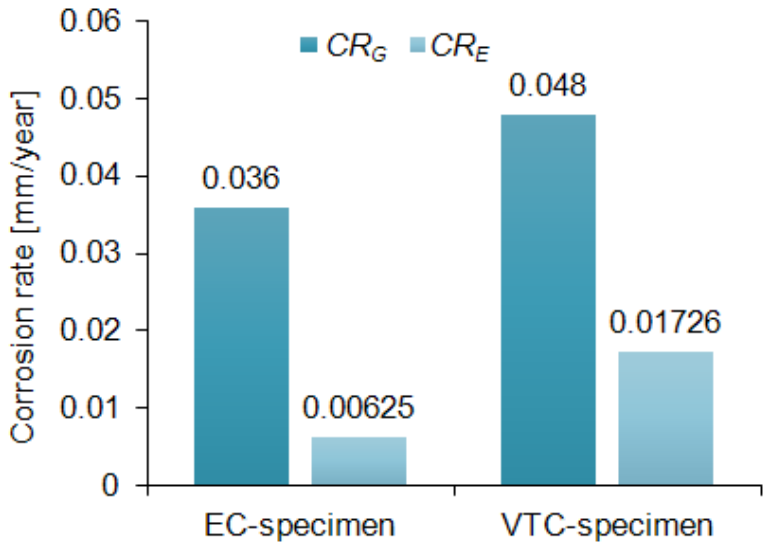

Figure 3. Gravimetric versus electrochemical corrosion rates for the emulsion cooled (EC) and the vortex tube cooled (VTC) X20Cr13 specimens.

The gravimetric and electrochemical corrosion rates are compared in Figure 3. As can be seen, the gravimetric corrosion rate of the EC-specimen was 5.76 times higher than the electrochemical one, but both were well below the permissible value of 0.1 mm/year. However, the gravimetric corrosion rate of the VTC-specimen was only 2.78 times higher than the electrochemical one. This is in consistent with the outcome of open circuit measurements and leads to an important conclusion that chilled air-cooling method in turning the tested material X20Cr13 has a beneficial effect on the corrosion resistance over a longer time period.

3.3. SEM/EDS Results

The intensity of passivation of stainless steels is most affected by the mass fraction of Cr. In most environments, Cr has the ability to form a stable and passive oxide film on the surfaces of stainless steels that protects them from further corrosion. The corrosion resistance is also influenced by the mass fraction of C. The higher it is, the greater the danger of carbide formations. If C is combined with Cr (chromium carbide) it may have a detrimental effect on corrosion resistance by reducing the amount of Cr available to ensure corrosion resistance property [26]. Therefore, it is desirable to have the highest possible Cr percentage and the lowest possible C content.

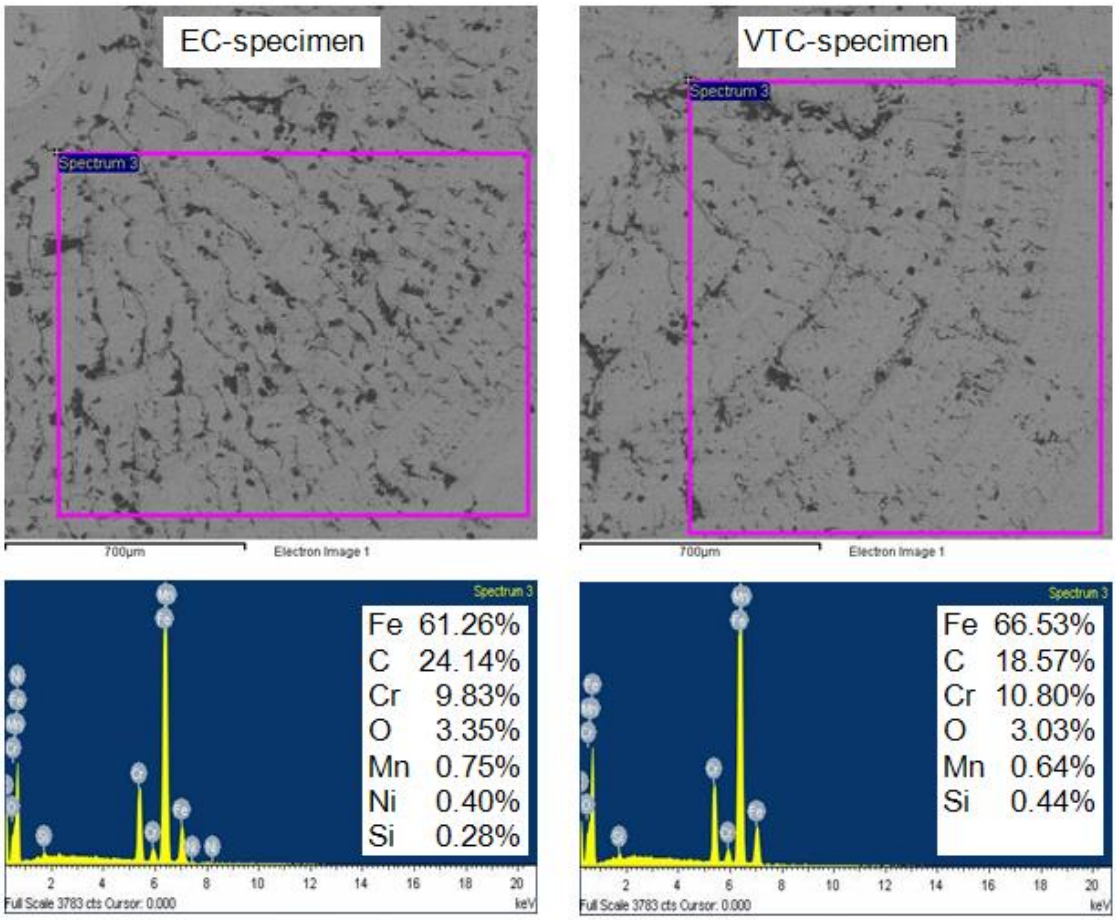

Figure 4. SEM/EDX results of the emulsion cooled (EC) and the vortex tube cooled (VTC) X20Cr13 specimens after being corroded in 3.5% NaCl aqueous solution at 25°C for 30 min.

SEM/EDS analysis was used to identificate the chemical elements and their percentages inside the observed surfaces on the specimens after corrosion testing in 3.5% NaCl aqueous solution at 25°C for 30 min. The results are shown in Figure 4. For the EC-specimen, the analysis confirmed the presence of Fe, C, Cr, O and less amounts of Mn, Ni, Si on the surface. The presence of O and C was an indication of oxides and carbides formation on the surface. Also, in a chloride environment, Ni could form a stable passive nickel oxide layer. For the VTC-specimen, the analysis confirmed the presence of all elements as for the EC-specimen with the exception of Ni.

In comparison to the EC-specimen, the VTC-specimen had more Cr, appreciably less C and slightly less O. Hence, it is reasonably to say that chilled air-cooling method in turning the tested material X20Cr13 does not degrade noticeably its corrosion resistance.

3.4. Machinability Results

After obtaining the *Ra* (mean roughness) data from the experiments, corresponding *S*/*N* ratios were calculated using Equation (3) as given in Table 7. Then, an average of the *S*/*N* ratios for each level of control factors individually was determined as listed in Table 8. The total mean of *S*/*N* ratios for 18 experiments is also listed. In order to determine the influence of each control factor on the *Ra*, a graphical analysis of data in Table 8 was performed using the main effects plot for *S*/*N* ratios shown in Figure 5.

Table 7. Experimental machinability results and corresponding *S*/*N* ratios.

Exp. No.	A: Cooling method	B: v_c [m/min]	C: f [mm/rev]	D: a_p [mm]	*Ra* [μm]	*S*/*N* [dB]
1	Emulsion	170	0.2	0.3	1.530	-3.69383
2	Emulsion	170	0.3	0.4	1.560	-3.86249
3	Emulsion	170	0.4	0.5	1.978	-5.92453
4	Emulsion	220	0.2	0.3	1.524	-3.66198
5	Emulsion	220	0.3	0.4	1.665	-4.42828
6	Emulsion	220	0.4	0.5	2.118	-6.51688
7	Emulsion	270	0.2	0.4	1.359	-2.66695
8	Emulsion	270	0.3	0.5	1.656	-4.38121
9	Emulsion	270	0.4	0.3	1.788	-5.04541
10	Chilled air	170	0.2	0.5	1.407	-2.96588
11	Chilled air	170	0.3	0.3	1.669	-4.44986
12	Chilled air	170	0.4	0.4	1.909	-5.61848
13	Chilled air	220	0.2	0.4	1.381	-2.80387
14	Chilled air	220	0.3	0.5	1.671	-4.45953
15	Chilled air	220	0.4	0.3	1.994	-5.99450
16	Chilled air	270	0.2	0.5	1.291	-2.21852
17	Chilled air	270	0.3	0.3	2.371	-7.49863
18	Chilled air	270	0.4	0.4	1.880	-5.48316

In Figure 5, the inclination angle of the line connecting different levels represents the influence of control factor on the *Ra*. It can be seen that the feed rate *f* (factor C) has the greatest influence in

reducing the *Ra* since it has the largest difference in the values of *S*/*N* ratio (between maximum and minimum), followed by depth of cut a_p (factor D), cutting speed v_c (factor B) and cooling method (factor A). However, accurate statistical and physical significance as well as the contribution of control factors should be established by analysis of variance (ANOVA).

Table 8. *S*/*N* response table (means).

Level	A	B	C	D
1	-4.46462	-4.41918	-3.00184	-5.05737
2	-4.61027	-4.64417	-4.84667	-4.14387
3	/	-4.54898	-5.76383	-4.41109
Total mean of *S*/*N* = -4.53744				

The degree of freedom *DF*, sum of squares *SS*, mean squares *MS* (variance), *F*-value (calculated variance ratio) and F_0-value (tabulated variance ratio) were determined along with a percentage contribution C_p of each source of variation. The ANOVA results are presented in Table 9. The C_p indicates the relative power of the source to reduce variation. The higher the C_p value, the more important is the contribution of source change.

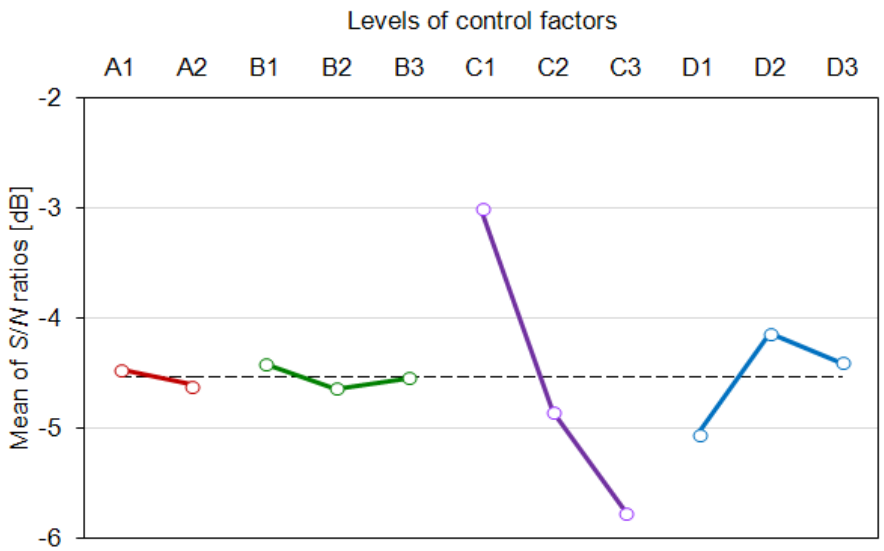

Figure 5. Main effects plot for *S*/*N* ratios.

Table 9. ANOVA results.

Source	*DF*	*SS*	*MS*	*F*-ratio	F_0-ratio	C_p [%]
A	1	0.09547	0.09547	0.109	$3.285_{(0.01,\,1,\,10)}$	0.27
B	2	0.15307	0.07653	0.088	$2.924_{(0.01,\,2,\,10)}$	0.43
C	2	23.74629	11.87314	13.573*	$2.924_{(0.01,\,2,\,10)}$	67.10
D	2	2.64710	1.32355	1.513	$2.924_{(0.01,\,2,\,10)}$	7.48
Error	10	8.74791	0.87479			24.72
Total	17	35.38983		*significant		

The ANOVA results indicate that the cooling method, v_c, f and a_p influence the *Ra* by 0.27%, 0.43%, 67.10% and 7.48%, respectively. Hence, the f is confirmed to be the most important factor affecting the *Ra*. According to Table 9, it can be said that the a_p, v_c and cooling method have no statistical and physical significance with respect to the *Ra* at the confidence level of 99% because their F-calculated values are less than corresponding F_0-tabulated values. The ANOVA also shows that the contribution of error is high (24.72 %), which distinctly suggests the existence of the interaction effects of control factors.

In the scope of this study, the most interesting finding is that about non-significant influence of the cooling method on reducing the *Ra* and consequently on increasing the corrosion resistance of machined surface. Therefore, the flood cooling with emulsion can be replaced with the chilled air-cooling using the vortex tube during turning the martensitic stainless steel X20Cr13 as the corrosion resistance remains unaffected.

4. CONCLUSIONS

The utilization of cutting fluids is commonly recommended in machining of martensitic stainless steels. The ever growing challenge to practise a green machining without sacrificing the machining performances direct the manufacturing industry to the development and implementation of the alternatives to conventional liquid coolants, which will not be a threat to the future or sustainability of machining. A chilled jet of compressed air is one such alternative. However, corrosion of the workpiece can occur even in dry machining when no cutting fluid is used. The presented study offers indispensable knowledge on the feasibility of replacing conventional emulsion coolant with the chilled air generated by the vortex tube, also taking into account the corrosion resistance of the martensitic stainless steel X20Cr13 after the turning operation. From the investigation results, the following conclusions can be summarized:

- According to open circuit potential measurements, the chilled air-cooling method provokes a delayed spontaneous creation and gradual thickening of the passive oxide film on the surface of tested material, which forms a protective layer, and the corrosion resistance is on increase over a longer time period.
- According to potentyodinamic polarization measurements, the emulsion cooled surface of tested material shows a lower corrosion predisposition.
- Comparison of gravimetric versus electrochemical corrosion rates confirms the outcome of open circuit measurements.
- According to SEM/EDS analysis, the chilled air-cooling method does not degrade noticeably the corrosion resistance of tested material.
- According to Taguchi analysis, the feed rate f has the greatest influence in reducing the surface roughness parameter *Ra*, followed by depth of cut a_p, cutting speed v_c and cooling method.
- According to ANOVA, the f is confirmed to be the most significant factor influencing the *Ra*, the a_p, v_c and cooling method have no statistical and physical significance, and an existence of the interaction effects of control factors is clearly indicated.

The most motivating discovery in the above findings is surely the non-significant influence of the cooling method on reducing the *Ra* and consequently on increasing the corrosion resistance of the machined surface. It greatly encourages the replacement of emulsion cooling with chilled air-cooling generated by the vortex tube. Therefore, the green turning of martensitic stainless steel X20Cr13 is feasible without sacrificing the machining performance and the ecological burden inherent in the conventional liquid coolant can be removed.

It would be of further interest to develop mathematical models, which describe the dependence of corrosion resistance on the roughness of machined surface with respect to the cooling methods. Besides, it is necessary to examine the impact of chilled air-cooling on the tool wear. At last, it would also be desirable to check the costs of introducing chilled air-cooling system.

ACKNOWLEDGEMENTS
This work was supported by the University of Rijeka, Croatia under Grant No. 13.09.1.2.10.

References

1. BSSA, General principles of machining stainless steels (2017). http://www.bssa.org.uk/topics.php?article=192 (accessed Nov 18, 2017).
2. M. Soković and K. Mijanović, *J. Mater. Process. Technol.,* 109 (1-2) (2001) 181.
3. G. Byrne, D. Dornfeld and B. Denkena, *CIRP Ann.,* 52 (2) (2003) 483.
4. S. Ueno, Y. Shiomi and K. Yokata, *Ind. Health,* 40 (2002) 291.
5. C. Mackerer, *Toxicol. Ind. Health,* 5 (1989) 429.
6. P.S. Thorne, J.A. DeKoster and P. Subramanian, *Am. Ind. Hyg. Assoc. J.,* 57 (12) (1996) 1163.
7. T.J. Bierma and F.L. Waterstraat, Total cost of ownership for metalworking fluids. Research report 105, Illinois Waste Management and Research Center, 2004.
8. V.P. Astakhov, Ecological machining: near-dry Machining. In *Machining: fundamentals and recent advances*; Davim, J.P., Ed.; Springer-Verlag (2008) London, pp 195-223.
9. F. Pusavec, D. Kramar, P. Krajnik and J. Kopač, *J. Cleaner Prod.,* 18 (12) (2010) 1211.
10. L. Celent, Implementation of compressed cold air using vortex tube in milling process. PhD Thesis, University of Split, FESB, Croatia, (in Croatian) (2014).
11. U.S. Dixit, D.K. Sarma and J.P. Davim, Environmentally friendly machining, Springer (2012) New York, USA.
12. J. Liu and Y.K. Chou, *Int. J. Mach. Tools Manuf.,* 47 (3-4) (2007) 635.
13. Y. Su, N. He, L. Li, A. Iqbal, M.H. Xiao, S. Xu and B.G. Qiu, *Int. J. Mach. Tools Manuf.,* 47 (6) (2007) 927.
14. B. Boswell, Use of air-cooling and its effectiveness in dry machining processes, PhD Thesis, Curtin University, Australia (2008).
15. V.S. Sharma, M. Dogra and N.M. Suri, *Int. J. Mach. Tools Manuf.,* 49 (6) (2009) 435.
16. N.M. Liu, K.T. Chiang and C.M. Hung, *Int. J. Adv. Manuf. Technol.,* 67 (5-8) (2013) 1053.
17. G. Foltz, Corrosion and metalworking fluids (2003). http://www.productionmachining.com/articles/corrosion-and-metalworking-fluids (accessed Nov 18, 2017).
18. L. Yang (Ed.) Techniques for corrosion monitoring, Woodhead Publishing (2008) Cambridge, UK.
19. N. Popov, Corrosion engineering: principles and solved problems, 1st ed.; Elsevier (2015).
20. ASTM G102-89. Standard practice for calculation of corrosion rates and related information from electrochemical measurements; ASTM International: West Conshohocken, PA, 2015e1.
21. ASTM G1-03. Standard practice for preparing, cleaning, and evaluating corrosion test specimens;

ASTM International: West Conshohocken, PA, 2011.
22. O. Zerti, M.A. Yallese, S. Belhadi and L. Bouzid, Taguchi design of experiments for optimization and modelling of surface roughness when dry turning X210Cr12 steel. In *Applied mechanics, behaviour of materials, and engineering systems*. Lecture Notes in Mechanical Engineering; T. Boukharouba, G. Pluvinage, K. Azouaoui, Eds.; Springer: Cham, (2017), pp 275-288.
23. R. Rashad, A.E. Amer, A.Y. Shash and H. Shendy, Effect of alloying elements on corrosion, microstructure and mechanical properties for casted free-nickel duplex stainless steels. In *Mechanical and materials engineering of modern structure and component design*; A. Öchner, H. Altenbach, Eds.; Springer: Switzerland, (2015); Advanced Structured Materials, Vol. 70, pp 1-11.
24. F.E.-T. Heakal and Kh.A. Awad, *Int. J. Electrochem. Sci*., 6 (2011) 6483.
25. X.G. Zhang, Corrosion and electrochemistry of zinc; Springer (1996) US.
26. B. Moisă, Influence of chemical composition on stainless steels mechanical properties, Proceedings of the 13th WSEAS International Conference MACMESE '11; M. Demiralp, Z. Bojkovic, A. Repanovici, Eds.; WSEAS Press: Stevens Point, 2011; pp 95-100.

© 2018 The Authors. Published by ESG (www.electrochemsci.org). This article is an open access article distributed under the terms and conditions of the Creative Commons Attribution license (http://creativecommons.org/licenses/by/4.0/).